

Design & Performance Analysis of Octagonal Hollow Core Photonic Crystal Fibers

Vidya Viswanathan
Department of Electronics and
Communication Engineering
SRM Institute of Science and
Technology, Kattankulathur
Chennai, India
vvidya.deepa@gmail.com

Chirag Goyal
Department of Electronics and
Communication Engineering
SRM Institute of Science and
Technology, Kattankulathur
Chennai, India
chiraggoyal34@gmail.com

Akanksha Verma
Department of Electronics and
Communication Engineering
SRM Institute of Science and
Technology, Kattankulathur
Chennai, India
vakanksha62@gmail.com

Abstract — Hollow core photonic crystal fibre can be designed in various shapes and orientations like hexagonal, octagonal and decagonal. This paper mainly emphasizes on design and development of octagonal hollow core photonic crystal fibre. Three different structures have been designed keeping the octagonal orientation of the air holes. Variations in the air hole diameter, along with radius of cladding is done. The fiber design consisting of air holes throughout the complete surface of the cladding in cylindrical geometry including a perfectly matched layer on the outer surface of the optical fiber. We propose to develop and design different photonic crystal fibers with change in optical parameters. The environment which we are using for design and development of photonic crystal fiber is Comsol Multiphysics 5.4 version. The electric field is integrated inside the fiber using mesh in the electromagnetic wave, frequency domain to obtain aggregate electric field. Variation is done with the different values of wavelength in the optical spectrum ranging from $1.2\mu\text{m}$ to $1.8\mu\text{m}$. The variation of different properties like pitch, diameter of the fibre, wavelength of the light in the optical spectrum, variation in arrangement of holes through cladding surface and different materials gives us the opportunity to utilize the photonic crystal fibers for specific applications. This inference can be made by using graphical analysis using the confinement loss, propagation constant, effective refractive index and attenuation constant obtained from various designs. The graphical analysis is done using the software ORIGIN 9.0. A brief comparison with the optical parameters is done with the fibers designed and the octagonal HC-PCF shows best results among all the designs made.

Keywords — Photonic crystal fiber, octagonal hollow core photonic crystal fiber, confinement loss, propagation constant, attenuation constant, anti-resonant reflection

I. INTRODUCTION

The conventional optical fibers are normal step index fibers which are having higher refractive index at the centre (core) and lower refractive index in cladding structure. This is employed for internally reflection based applications. Fibers which possess guided modes have refractive index among core and cladding. Fig.1 refers to the structure of an optical fiber, consisting of core, cladding and the outer protection jacket from environmental factors which could affect the functioning. With further development in optical fibers, photonic crystal fibers was found in the year 1996. The fiber consists of a core which is solid where the air holes are spaced in a hexagonal manner throughout the fiber which

would help in light confinement in the central part known as core of the photonic crystal fiber. These optical fibers contain a micro-structured arrangement of different materials of different refractive indices. There are guiding mechanisms used in photonic crystal fibers namely index guiding mechanism and photonic band-gap mechanism. The space filling mode determines the effective values of refractive index obtained of the cladding. Some of desirable properties of photonic crystal fiber are non-linearity, mode transmission via single means, dispersion that can be tuned and higher birefringence. Dispersion compensation modules also called dispersion compensation units which are utilized for compensating chromatic dispersion. Single mode allows selective transmission, redirects or blocks an optical signal in a transmission medium which can be used over longer distances. When the polarization modes propagate with different velocities and their difference between the values of refractive indices is called birefringence [4]. The phase difference between the two modes of the fiber is an integral multiple of 2π , the two modes will beat at this point and input polarization will be reproduces.

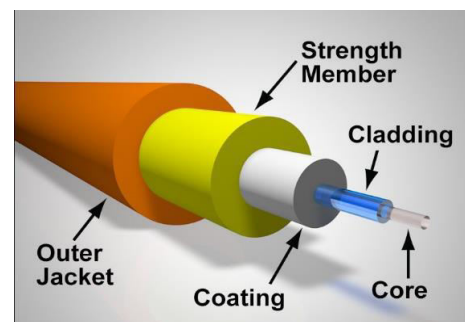


Fig.1 Structure of optical fiber

The photonic crystal fibers were eventually succeeded by cylindrical Bragg's waveguide, which consists of Silicon Carbide (SiC) core surrounded by alternate silicon (Si) and silicon oxide (SiO₂) layers in the cladding. These layers consist of low and high refractive index material rings. The waveguide uses forbidden gap for light confinement within the core of fiber having lower index value. In band-gap certain frequencies cannot propagate. Effective refractive index values of fundamental range of core, mode will reside within the provided band-gap [9]. Hollow core photonic band-gap fibers reduces loss of

transmission, low non-linearity and higher values of threshold which could lead to damage. Central core of the fiber that is responsible for light confinement could be made occupied with any known gas or other materials that leads for longer interaction length. Introduction of Kagome fibers accounted for lower losses during transmission.

The first theoretical demonstration of out of plane photonic band gap fiber was introduced in 1995. In 1999, the first hollow core photonic crystal fibers got developed [10]. This proved to be milestone in optical fiber history which had characteristics that could overcome the shortcomings of the existing fibers. It reduced transmission losses, possessed higher damage threshold and lower non linearity. First low loss and applied HC-PCF fiber was introduced in 2002. The first photonic microcell was developed in 2005. Kagome fiber accomplished lower losses in transmission of data with an air core. Anti-resonant reflection optical waveguide, also known as ARROW confines light in regions with comparatively lower refractive index [7]. Further research on anti-resonant reflection waveguide along with kagome fibers led to the discovery of negative curvature fibers.

The paper is divided into six sections. The section I gives a brief introduction and history of optical fibers and its evolution. Section II depicts the related work done till now in the field of photonic crystal fibers, their modifications and the design using different parameters. Section III represents the design and development of hollow core photonic crystal fibers, their specifications used in software and material used for analysis. Section IV shows the results obtained from the different hollow core photonic crystal fiber designs for graphical plots and performance analysis. Section V gives conclusion and section VI are the references used.

II. RELATED WORK

The papers present the evolution and improvement of optical fibers for various applications. Various parameters are taken into consideration for comparison and analysis is done with the help of Comsol Multiphysics software [14]. Research shows various geometrical designs like square, circular, and hexagonal structures. This is done for wavelength values from 800nm to 1600nm for studying optical parameters and variations in the properties. The three designs utilized for comparing the parameters like area effective, loss of light confinement [1] and wave guide dispersion. The material employed here is silica glass and the cladding region is mainly made up of four air holes. Effective area covers those dimensions which are transverse of the fiber. Propagation constant measures the changes occurred in the amplitude values of the wave as it propagates in a given direction. The loss which is caused by the arrangement of air holes in the cladding surface is known to be called as confinement loss. If the fraction of light power that is travelling pass through the cladding is comparatively more efficient and faster than the core region, then dispersion in waveguide [5] tends to occur. The PCF's are designed with single material. The air holes are present around the core in the form of many rings. PCF's have greater advantage than classical fibers. Wider range of wavelength of single mode guidance, dispersion, non-linearity and birefringence control [15].

Core of the PCF can be solid or hollow in structure [2]. PCF's with solid core have the light travelled by the changed total internal reflection and on the other hand in case of hollow core, the propagation of light is through the principle of photonic band-gap. In the solid core fibers, the cladding has lower refractive index than the core which is known as index-guiding. FSM mode is the fundamental mode which propagates in the cladding. Numerical and analytical methods can be used for calculation and analysis of FSM. Analytical methods are of two types: scalar and vectoral [6]. Vectoral methods are better. Single mode is guided in the core of PCF. Low order modes and effective indices were obtained in cladding of PCF. In the FSM layer, maximum effective refractive index of the PCF modes have been observed. Lowest wavelength is obtained at 560nm, cutoff wavelength is core fundamental guided mode.

III. HOLLOW CORE PHOTONIC CRYSTAL FIBER DESIGN

The fiber is designed with octagonal oriented air holes which passes throughout the cladding surface. Parameters taken are pitch = $0.7[\mu\text{m}]$, diameter of air holes = $0.7 * p [\mu\text{m}]$, radius of core = $d/2$, input wavelength = $1.55[\mu\text{m}]$, thickness of perfectly matched layer = $5[\mu\text{m}]$, radius of cladding = $8 * p [\mu\text{m}]$. These are the parameters for the first design made in Comsol Multiphysics. Fig.2 (a) represents the structure of octagonal HC-PCF with the first design parameters given as input in Comsol Multiphysics 5.4. The structure has 4 consecutive rings of air holes with silica glass in the cladding structure and perfectly matched layer. Apart from this, an octagonal HC-PCF is designed by changing air hole diameter holes keeping other parameters same. Change in the radius of cladding = $10 * p [\mu\text{m}]$ and thickness of perfectly matched layer = $3[\mu\text{m}]$, another octagonal HC-PCF is designed. In all the three designed structures, silica glass is used as a material in the perfectly matched layer and the cladding and air is used as a material in the air holes. The analysis is done using Comsol Multiphysics 5.4 under the optical window of $1.2\mu\text{m} - 1.8\mu\text{m}$. The reason for choosing this range is that it constitutes the Mid-IR region of the spectrum as the optical communication ranges from 5nm (UV) to 1mm (IR) [11]. Longer wavelength band consisting of $1.2\mu\text{m}$ to $1.675\mu\text{m}$ offers superlative performance. Changing the size of air hole, pitch of air hole, shape of their structure [13] and diameter of air holes leads to zero dispersion wavelength taken for a wider range of values in near IR and visible spectrum.

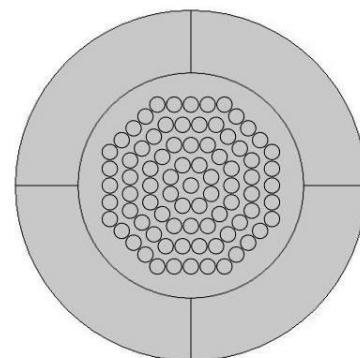


Fig.2 (a): Structure of octagonal HC-PCF when first design parameters are taken

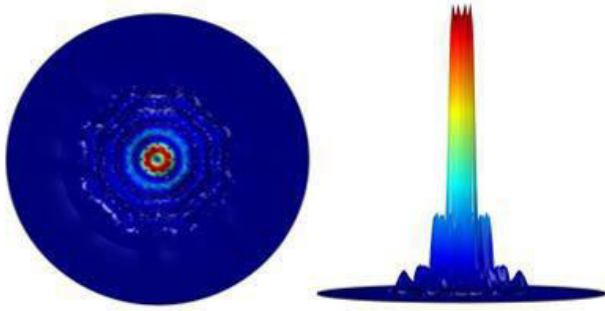


Fig.2 (b): XY and YZ plot of octagonal HC-PCF with first design parameters at $\lambda = 1.6\mu\text{m}$

Fig.2 (b) shows us the XY and YZ plot obtained when the octagonal HC-PCF is at a wavelength of $1.6\mu\text{m}$ in study mode analysis. The 3-D plot of the Gaussian field gives the study of distribution of light through the fiber.

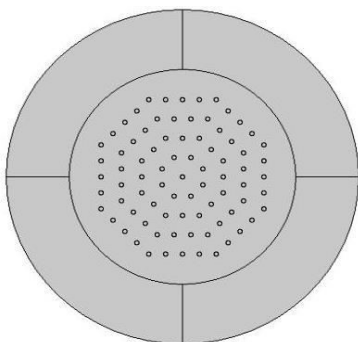


Fig.3 (a): Structure of octagonal HC-PCF with change in hole diameter

Fig.3 (a) depicts the schematic structure of octagonal HC-PCF with all the parameters given same as the octagonal HC-PCF as in previous case except the diameter of air holes. The material in the background used is silica glass for both cladding surface and perfectly matched layer.

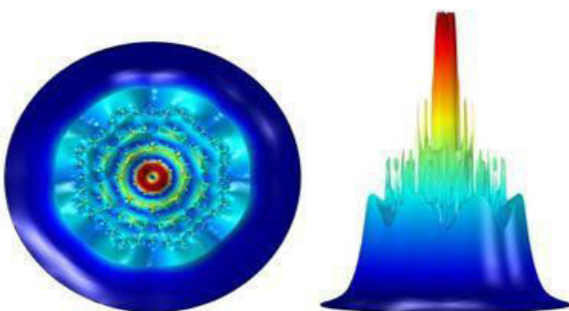


Fig.3 (b): XY and YZ plot of octagonal HC-PCF with change in air hole diameter in the cladding

Fig.3 (b) The YZ graph clearly shows the confinement with losses in 3-D Gaussian plot for the octagonal HC-PCF with the change in air hole diameter throughout the cladding. The XY plot shows the top view of the fibers' best confinement at wavelength of $1.77\mu\text{m}$.

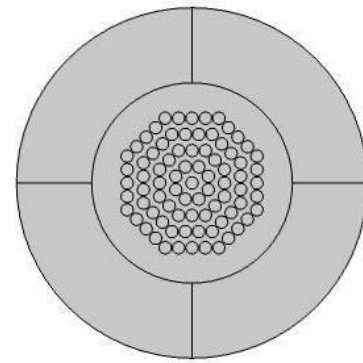


Fig.4 (a): Structure of octagonal HC-PCF with change in thickness of PML and radius of cladding

Fig.4 (a) shows the diagrammatic representation of octagonal HC-PCF with the change in thickness of perfectly matched layer and the radius of cladding is given to be 10 times the pitch. Pitch can be defined as the distance across the centres of two consecutive holes keeping all other input parameters same as that of octagonal HC-PCF originally except the above mentioned.

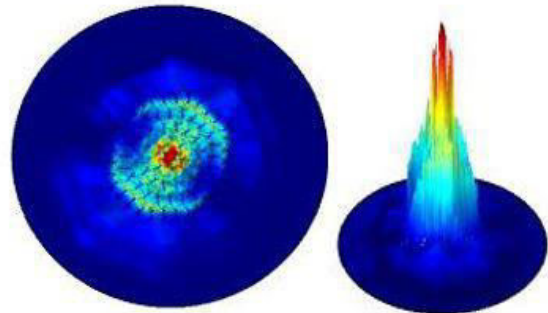


Fig.4 (b): XY and YZ plot of octagonal HC-PCF with change in in thickness of PML and radius of cladding

Fig.4 (b) represents the top view in XY plot which shows the light confinement at wavelength at $1.56\mu\text{m}$. YZ plot shows the Gaussian wave at the same wavelength after which the global evaluation is performed to match with the best and nearest value of effective refractive index obtained.

IV. RESULTS AND DISCUSSION

Computation is done with various effective values of refractive indices by changing values of wavelength in study mode analysis. The structure is built in mesh wherein the electric field is calculated using integration over a given surface. After the fundamental mode is found out by varying the values in effective mode index, the Gaussian wave with the best confinement is chosen. Global evaluation is done and expression for electromagnetic waves, frequency domain – attenuation constant per meter dB is fed as input. After the global evaluation, a new table is obtained. The nearest value of the refractive index is found and noted down. Values of effective refractive index consists of real part and imaginary part. We also find out values for attenuation

constant corresponding to different values of wavelength. Graphical analysis is done by plotting following graphs: a) real part of refractive index and wavelength, b) propagation constant and wavelength, c) confinement loss and wavelength, d) attenuation constant and wavelength. The confinement loss depends on imaginary value of effective refractive index. Waveguide dispersion, propagation constant and effective area depends on the real part of refractive index. The change faced by the fiber when it propagates in a given direction, in amplitude is called propagation constant.

$$\beta = (\eta_{eff}) \times \left(\frac{2\pi}{\lambda}\right) \tag{1}$$

where η_{eff} is effective refractive index, λ is input wavelength. Equation (1) shows the mathematical representation of propagation constant. The loss in light confinement which is caused due to the periodic arrangement of the cladding in the photonic crystal fiber is known as the confinement loss. It is denoted by L_c . Equation (2) denotes the confinement loss formula.

$$L_c = 8.686 \times k_0 \times Im(\eta_{eff}) \tag{2}$$

Where $k_0 = (2\pi/\lambda)$ and $Im(\eta_{eff})$ is imaginary part of effective refractive index.

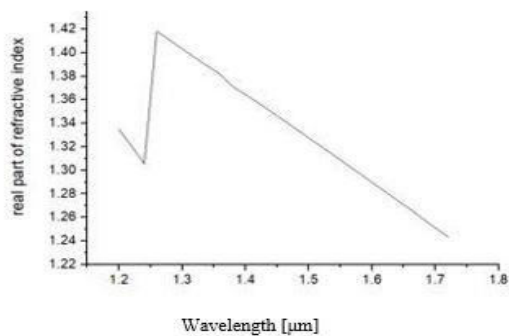


Fig.5 (a): Plot of real part of refractive index and wavelength for octagonal HC-PCF with first design parameters.

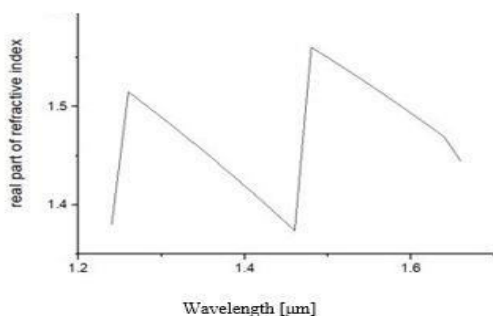


Fig.5 (b): Plot of real part of refractive index and wavelength for octagonal HC-PCF when air hole diameter is varied.

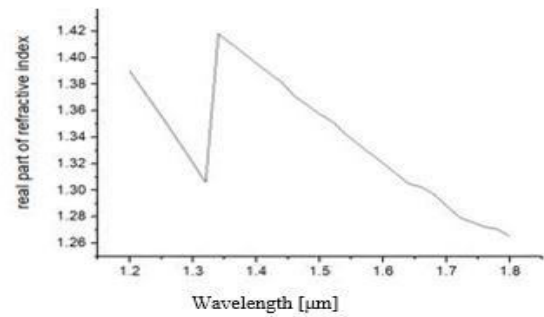


Fig.5 (c): Plot of real part of refractive index and wavelength for octagonal HC-PCF when thickness of PML and radius of cladding is varied.

Fig.5 represents the graphical plot of real part of refractive index and the wavelength [μm]. Optical parameters namely waveguide dispersion and effective area depend directly on real part of refractive index. Fig.5 (a) we infer that with increase in wavelength, initially the peak is obtained at around $\lambda=1.3\mu m$, then decreases sharply. Fig.5 (b) shows two distinct peaks at $\lambda=1.3\mu m$ and $\lambda=1.55\mu m$ when the design involves change in diameter of air holes. Fig.5 (c) the peak is obtained around $\lambda=1.4\mu m$ and with further increase in wavelength we observe a decreasing trend in curve when the thickness of PML and radius of cladding is varied.

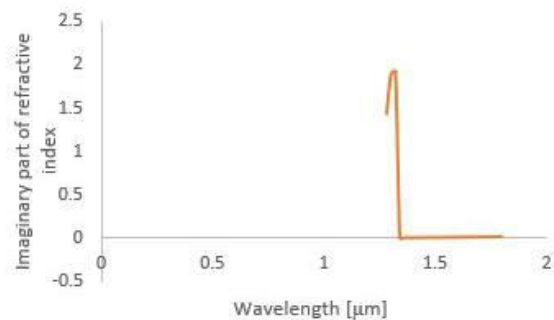


Fig.6 (a): Plot of imaginary part of refractive index and wavelength for octagonal HC-PCF with first design parameters

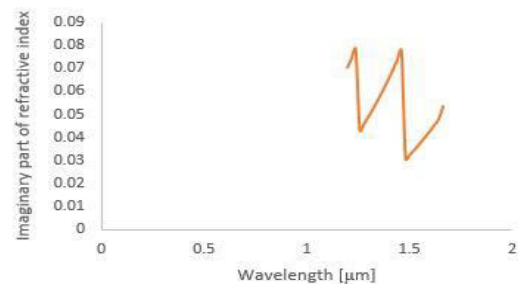


Fig.6 (b): Plot of imaginary part of refractive index and wavelength for octagonal HC-PCF when air hole diameter is varied.

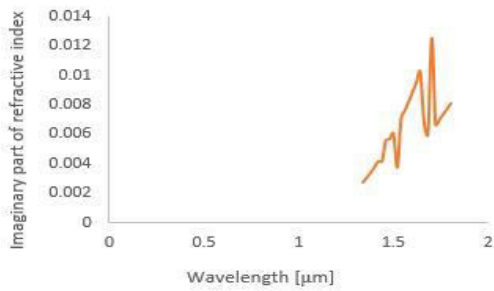


Fig.6 (c): Plot of imaginary part of refractive index and wavelength for octagonal HC-PCF when thickness of PML & radius of cladding is varied

Fig.6 represents the graphical plot of imaginary part of refractive index and the wavelength [μm]. Optical parameters namely confinement loss depend directly on imaginary part of refractive index. Fig.6 (a) we infer that with increase in wavelength, initially the peak is obtained at around $\lambda=1.35\mu m$, then decreases sharply. In Fig.6 (b) and Fig.6(c) there is a varying plot. Imaginary part of effective refractive index also depends on amount of absorption, which is a major factor for attenuation. So, the Fig.6 (a) gives the optimum result.

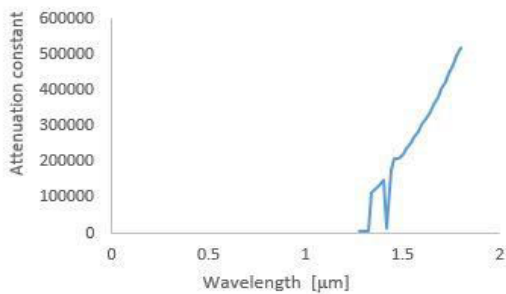


Fig.7 (a): Plot of attenuation constant and wavelength for octagonal HC-PCF with first design parameters

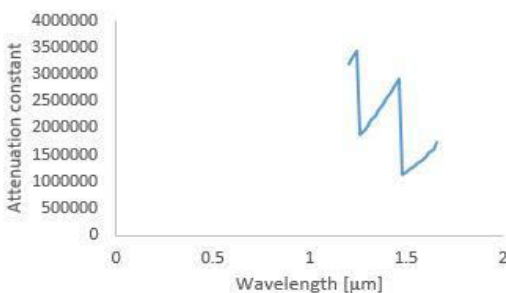


Fig.7 (b): Plot of attenuation constant and wavelength for octagonal HC-PCF when air hole diameter is varied

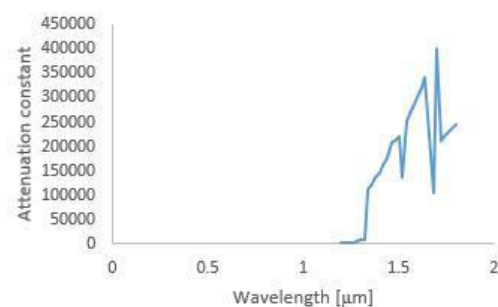


Fig.7 (c): Plot of attenuation constant and wavelength for octagonal HC-PCF when thickness of PML and radius of cladding is varied.

Fig.7 attenuation constant vs wavelength [μm] plot. Fig.7 (a) we note that with wavelength increase peak is obtained at a $\lambda=1.8\mu m$. In Fig.7 (b) there is a sharp decrease observed initially, then sudden increase. Further increase in wavelength there is an increase observed. The peak is around $\lambda=1.3\mu m$. Fig.7(c) shows an overall increasing trend up to $\lambda= 1.7\mu m$. Ideally, it is observed that with increasing wavelength, the attenuation constant tends to increase. Therefore, for practical applications lower wavelengths can be preferred.

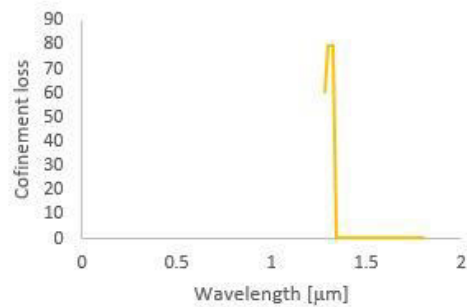


Fig.8 (a): Plot of confinement loss and wavelength for octagonal HC-PCF with first design parameters

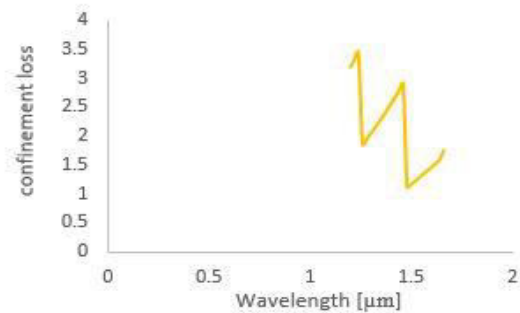


Fig.8 (b): Plot of confinement loss and wavelength for octagonal HC-PCF when air hole diameter is varied.

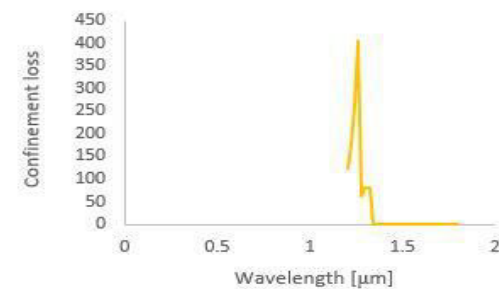


Fig.8 (c): Plot of confinement loss and wavelength for octagonal HC-PCF when thickness of PML and radius of cladding is varied.

Fig.8 is the graphical plot between confinement loss and the wavelength [μm]. From the above graphs, we can see that confinement loss is the least towards the end of the optical spectrum window. The Fig.8 (a) is the most desirable and has less variable losses among the above present. Fig.8 (b) shows a varied plot and Fig.8 (c) has a distinct peak nearly at $\lambda= 1.25\mu m$.

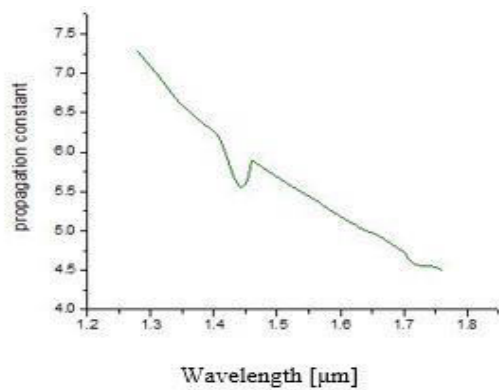


Fig.9 (a): Plot of propagation constant and wavelength for octagonal HC-PCF with first design parameters

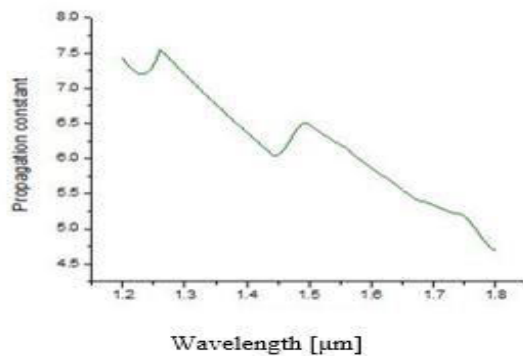


Fig.9 (b): Plot of propagation constant and wavelength for octagonal HC-PCF when air hole diameter is varied.

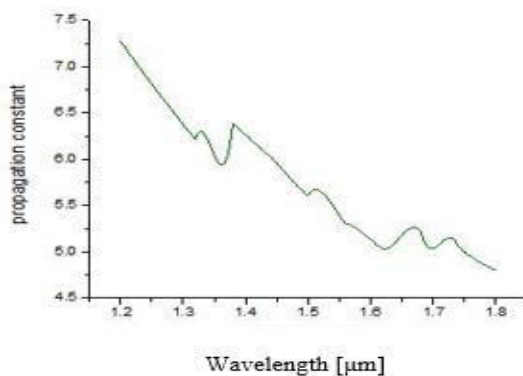


Fig.9 (c): Plot of propagation constant and wavelength for octagonal HC-PCF when thickness of PML and radius of cladding is varied.

Fig.9 represents the graphical plot of propagation constant and the wavelength [μm]. In all the three graphs a decreasing trend is observed. This is due to the fact that wavelength is inversely proportional to the propagation constant. Fig.9 (a) has the least variations compared to Fig.9 (b) and Fig.9 (c). Thus signifies the variation of the amplitude as the wave propagates in a particular direction.

V. CONCLUSION.

As it is known that hollow core photonic crystal fibers are far better than the conventional optical fibers, that mainly work on photonic bandgap mechanism. The fact that it utilizes photonic bandgap gives us the opportunity to make optimum use of the limited spectrum available to the best possible use. The graphical analysis of all the three octagonal hollow core photonic crystal fibers

designs for various optical parameters like real part & imaginary part of effective refractive index, attenuation constant, confinement loss and propagation constant is implemented successfully. From the results obtained, we conclude that the octagonal hollow core photonic crystal fiber with silica glass material with given input parameters; pitch = $0.7[\mu\text{m}]$, diameter of air holes = $0.7 \cdot p [\mu\text{m}]$, radius of core = $d/2$, input wavelength = $1.55[\mu\text{m}]$, thickness of perfectly matched layer = $5[\mu\text{m}]$, radius of cladding = $8 \cdot p [\mu\text{m}]$ gives the most efficient and optimized model for practical application usage among the three design structures. The application can be extended to data communication and data transfer in the conventional band and long band optical spectrum which ranges from $1.53\text{-}1.62\mu\text{m}$. Other applications include surgical procedures, surveillance, sensing [12], micromaching, terahertz communication [3]. This is because, this design gives least deviation in confinement loss along with propagation constant graphical plots which decreases steadily with increase in wavelength. The research and development of the fiber design is not only limited to using one material in the background but also takes the chance to utilize other materials like borosilicate, fused silica, silicon doped with fluorine. Doping concentration can be also done using materials like gold and silver. Variations in the shape of the air holes itself and its orientation structure can also be implemented for further development. There are many other optical parameters that can be taken into consideration for analysis like sensitivity [8], coupling length, birefringence, dispersion and many others.

VI. REFERENCES

- [1] Qin, Y., Jiang, P., Yang, H., Niu, Y., & Gui, F. (2019, January). Broadband and low confinement loss photonic crystal fibers supporting 48 orbital angular momentum modes. In *Third International Conference on Photonics and Optical Engineering* (Vol. 11052, p. 110520S). International Society for Optics and Photonics.
- [2] Habib, M. S., Antonio-Lopez, J. E., Markos, C., Schülzgen, A., & Amezcu-Correa, R. (2019). Single-mode, low loss hollow-core anti-resonant fiber designs. *Optics Express*, 27(4), 3824-3836
- [3] Islam, M. S., Sultana, J., Rifat, A. A., Dinovtser, A., Ng, B. W. H., & Abbott, D. (2018). Terahertz sensing in a hollow core photonic crystal fiber. *IEEE Sensors Journal*, 18(10), 4073-4080.
- [4] Md. Bellal Hossain, Abdullah Al-Mamun Bulbul, Md. Abdul Mukit, Etu Podder. (2017). Analysis of Optical Properties for Square, Circular and Hexagonal Photonic Crystal Fiber. *Optics and Photonics Journal*, 2017, 7, 235-243
- [5] Rana, S., Rakin, A. S., Hasan, M. R., Reza, M. S., Leonhardt, R., Abbott, D., & Subbaraman, H. (2018). Low loss and flat dispersion Kagome photonic crystal fiber in the terahertz regime. *Optics Communications*, 410, 452-456.
- [6] Masum, B. M., Aminossadati, S. M., Leonardi, C. R., Kizil, M. S., & Amanzadeh, M. (2018). Numerical analysis of gas diffusion in drilled Hollow-Core Photonic Crystal fibres. *Measurement*, 127, 283-291.
- [7] Carter, R. M., Yu, F., Wadsworth, W. J., Shephard, J. D., Birks, T., Knight, J. C., & Hand, D. P. (2017). Measurement of resonant bend loss in anti-resonant hollow core optical fiber. *Optics express*, 25(17), 20612-20621.
- [8] Paul, B. K., Ahmed, K., Asaduzzaman, S., & Islam, M. S. (2017). Folded cladding porous shaped photonic crystal fiber with high sensitivity in optical sensing applications: design and analysis. *Sensing and Bio-Sensing Research*, 12, 36-42.

- [9] Luan, N., & Yao, J. (2017). A hollow-core photonic crystal fiber-based SPR sensor with large detection range. *IEEE Photonics Journal*, 9(3), 1-7.
- [10] Roth, P., Frosz, M. H., Günendi, M. C., & Russell, P. S. J. (French). (2017). Analytical formulation for bend loss in photonic crystal fibers with a single-ring hollow-core. *Research on Photonics*, 5(2), 88-91.
- [11] Bradley, T. D., Wheeler, N. V., Hayes, J. R., Gouveia, M. A., Liang, S., Chen & Richardson, D. J. (French). (2017). Low-loss Kagome hollow-core fibers from near-to-mid-IR operating. *Letters from Optics*, 42(13), 2571-2574.
- [12] Morshed Monir, Md. Faizul Huq Arif, Kawsar Ahmed, Sayed Asaduzzaman, (2016). Photonic Crystal Fiber design and optimization for liquid sensing applications. *Photonic / Vol sensors* 6, No 3, from 279 to 288.
- [13] Priyanka Arora, Mayank Joshi, December 2015. Comparative study of hybrid Hexagonal PCF structure on Dispersion and Confinement Loss at different pitch of Air holes. ISSN: 2321-0869 (O) 2454-4698 (P).
- [14] Seyhan Coskun, Yavuz Ozturk, Gokalp Kahraman, (2016). A study on parameters of Photonic Crystal Fiber Modes. *Reserch Gate*.
- [15] Pranaw Kumar, Manish Kumar Jaiswal, (2015), Multi-core Photonic crystal fiber with anomalous Dispersion behavior. *International Conference on Communication and Signal Processing*.